JOURNAL OF GEOPHYSICAL RESEARCH, VOL. 106, NO. D14, PAGES 15,053–15,063, JULY 27, 2001

Airborne measurements of tropospheric ice-nucleating aerosol particles in the Arctic spring

David C. Rogers,[1] Paul J. DeMott and Sonia M. Kreidenweis

Department of Atmospheric Science, Colorado State University, Fort Collins, Colorado

Abstract. Instrumented aircraft flights were made during field experiments in the Arctic Ocean, the NASA FIRE Arctic Cloud Experiment and SHEBA (Surface Heat Budget of the Arctic). Airborne measurements of ice nucleating aerosol particles (IN) used a continuous flow diffusion (CFD) chamber, covering -10° to -30°C and humidities from ice saturation to water supersaturation. During selected time periods, ice crystals that grew on ice nuclei in the chamber were sampled onto electron microscope (EM) grids for later examination of the nucleating particles. Samples of total aerosol (IN and non-IN) were also collected for comparative analyses. Concentrations of IN ranged from zero to rare very high values (hundreds per liter at -25°C), making the frequency distribution of IN highly skewed: when accumulated as 10 s average concentrations (volume ~0.17 L), 50% were zero. Additional evidence of few IN was seen in thin low-level stratus clouds at -10° to -20°C that persisted for several days with low concentrations of ice crystals (~0.1 L^{-1}) and a few tenths g m^{-3} liquid water. On occasion, small regions of high IN concentrations (hundreds per liter) were detected near the surface. The EM analyses indicated that ice nuclei a few tenths micrometer in size contained crustal materials (primarily Si) and had widely varying morphology. Many IN particles produced weak or no X-ray signatures, suggesting a dominant low-molecular-weight component not detected by the energy dispersive X-ray (EDX) system, and were probably carbonaceous. In contrast, for the total aerosol, S or S and Si were dominant components, and few particles had no X-ray signature.

1. Introduction

Studies of the earth's climate system indicate that clouds are a major modulating influence. Many cloud processes, however, are not well understood, in particular, the role of ice nucleating aerosol particles (IN, or ice forming nuclei, IFN) for ice formation. It is known that water clouds, ice clouds and mixed phase clouds have substantially different microphysical and radiative properties [*Curry et al.*, 1996; *Fowler and Randall*, 1996; *Baker*, 1997]. It is likely that the abundance and characteristics of ice nuclei can influence the concentration, shape and phase of cloud particles, the size and persistence of clouds, precipitation efficiency, and radiative exchange processes.

Two important aspects of the effects of clouds on the Earth's climate system have received considerable attention recently: changes in cloud reflectivity due to changes in cloud particle size [*Twomey*, 1977; 1991], and changes in cloud lifetime due to changes in precipitation efficiency, also induced by cloud particle size changes [*Albrecht*, 1989]. These effects focus on warm clouds and link the cloud microphysical changes to perturbations in abundance of cloud condensation nuclei (CCN). Analogous relationships have been postulated for Arctic stratus clouds and climate by *Curry et al.* [1996], and include possible effects from changes in CCN and ice nuclei. The goal of the research described in this paper is to improve the understanding of the sources, chemical nature, distribution and activation processes of Arctic IN. Measurements of IN are crucial to understanding ice formation in Arctic cloud systems and to considering whether anthropogenic effects have the potential to modify natural cloud processes.

1.1. Ice Nucleation Processes

The formation of ice in clouds can occur through several mechanisms including nucleation processes or interactions of cloud particles with pre-existing ice. The nucleation processes can be further divided into homogeneous (involving only water substance) or heterogeneous (involving reactions with aerosol particles). Homogeneous freezing of liquid water depends on the mass of liquid water and its temperature; in general, pure water will spontaneously freeze near -40°C. Haze drops that grow from sulfuric acid drops or deliquesce on soluble CCN may supercool below -40°C because the solute lowers the freezing point [e.g., *Chen et al.*, 2000].

Four heterogeneous nucleation mechanisms are distinguished for atmospheric ice formation [*Vali*, 1985]: deposition (or sorption, where the ice phase forms below water saturation), condensation freezing (the ice phase forms as supercooled liquid water condenses on CCN), contact freezing (a supercooled cloud droplet freezes when it is contacted by an ice nucleating aerosol), and immersion freezing (an ice nucleating aerosol is already immersed in a supercooled droplet, and the droplet freezes when it cools sufficiently).

1.2. Ice Particles and Aerosols in the Arctic

In aircraft studies of Arctic stratus clouds, *Jayaweera and Ohtake* [1973] found that ice crystal concentrations were generally low (~0.005 to 0.3 L^{-1}, -5° to -20°C), there was no evidence of ice crystal "multiplication." They found general agreement

[1] Now at NCAR Research Aviation Facility, Broomfield, Colorado.

Paper number 2000JD900790.
0148-0227/01/2000JD900790$09.00

between the concentrations of ice crystals and IN measurements using a settling cloud chamber and filter technique from a nearby surface site or Arctic baseline IN data [*Bigg and Stevenson,* 1970].

Observations of "diamond dust," or clear sky ice crystal precipitation, were made by *Ohtake et al.* [1982] along the coast of northern Alaska at the surface and from aircraft during late March. Ice crystals formed at low altitudes, ~-25°C over regions of open water, where the humidity was between ice and water saturation. Concentrations were ~1-30 L^{-1}. The crystals were small (typically < 100 μm), and their shapes indicated they formed first by condensation into droplets which subsequently froze. *Curry et al.* [1990] presented data from Arctic flights showing extensive ice cloud regions were often encountered, especially at low altitudes (in excess of 80% of flight time for five April flights).

The phenomenon of Arctic haze occurs in extensive and persistent layers during winter and is associated with intrusions of polluted air masses [*Schnell,* 1987; *Barrie,* 1986; *Brock et al.,* 1989]. This pollution is widespread, layered, and characterized by enhanced levels of carbon, particle concentration and mass loading. In airborne studies of Arctic aerosol, *Radke et al.* [1984] reported a peak at ~0.1-0.3 μm and typical total concentration of ~300 cm^{-3}. Arctic haze is an important component of the polar radiation budget because it covers large areas and persists for long periods. It clearly has an impact on the properties and processes in winter Arctic clouds [*Shaw et al.*, 1993]. *Borys* [1989] studied the IN properties of aerosols in regions with Arctic haze. Membrane filter samples were collected from aircraft at altitudes from the surface to the tropopause over long transects from Alaska to Greenland. He found that the western Arctic had fewer IN and was generally more polluted (higher CN and more industrial-source metal compounds) than the eastern Arctic. Typical IN concentrations at -15°C were very low, at or near the unexposed filter background (~0.1 to 5 L^{-1} at -25°C). Borys concluded that the Arctic haze aerosol had a lower fraction of IN and would not efficiently form ice in Arctic clouds. He also suggested that the relative decrease occurred due to deactivation of IN by sulfate coatings. This lack of an effective ice nucleation scavenging mechanism may be an important factor in the long range transport of Arctic haze.

Surface measurements of IN were made by *Radke et al.* [1976] during March 1970 near Barrow, Alaska, using a mixing chamber [*Langer*, 1973] at –20°C and yielded IN concentrations from 0.01 to 20 L^{-1}. *Fountain and Ohtake* [1985] made surface IN filter measurements in Alaska from June 1978 to March 1979. Their IN concentrations were based on 20 min samples and showed ~0.1 to 0.5 L^{-1} at -20°C and water saturation. *Bigg* [1996] measured IN from an ice breaker ship during the summer to fall transition. His IN measurements used the membrane filter technique, with sample times of 60 min. The filters were processed at -12.5°, -15°, and -17.5°C and showed concentrations ~0.01 L^{-1} in mid-summer decreasing to ~0.001 in early fall. Air trajectory analyses showed that higher IN concentrations were associated with passage over nearby open water areas and suggested that the ocean surface might be an IN source.

In general, IN concentrations reported for the Arctic have been less than those from midlatitude continental surface locations, where typical values are ~0.1 L^{-1} at -10°C increasing to ~5 L^{-1} at -20°C [e.g., summarized by *Cooper*, 1986] and up to ~100 L^{-1} at -30°C in the upper troposphere [*Rogers et al.*, 1998]. Arctic IN concentrations have also been lower than those from tropical and midlatitude maritime samples. For example, *Rosinski et al.* [1986, 1987] collected particles with size-segregated im-

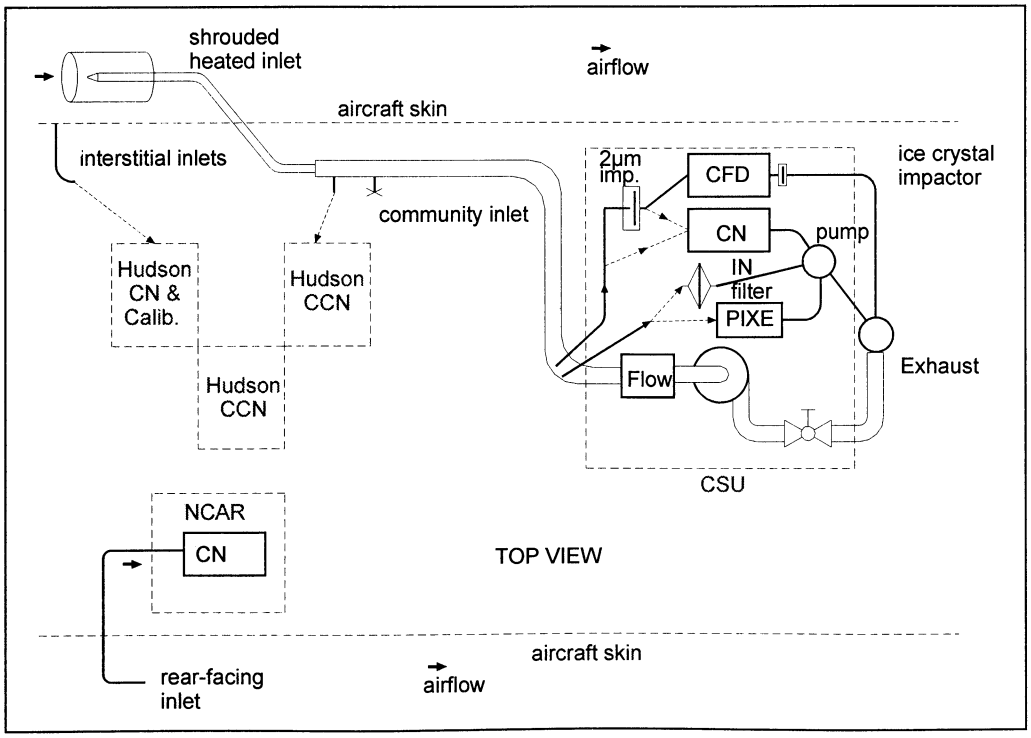

Figure 1. Distribution of air for ice nuclei (IN), condensation nuclei (CN) and cloud condensation nuclei (CCN) sampling on NCAR C-130 during May 1998 flights. Note 2 μm impactor upstream of continuous flow diffusion (CFD) chamber and ice crystal impactor downstream.

pactors and filters during cruises in the Pacific Ocean from 40°N to 60°S. These samples were analyzed from -3° to -17°C and from ice saturation to 2% supersaturation with respect to water (SS_w). They found essentially no activation by deposition (sorption) and high concentrations of IN activating by condensation freezing, 0.1 L^{-1} at -3.3° and 30 L^{-1} from -4° to -14°C. The fraction of particles active by condensation freezing was 0.001. Of particular interest, they found (1) the warmest IN were in a latitude band along the equator, (2) IN concentrations were as large as 40 L^{-1} at -4°C and did not increase at colder temperatures, and (3) particles supplying the IN were smaller than 0.5 μm diameter and seemed to consist mostly of organic matter. The oceanic region of high IN concentrations was associated with upwelling and biological activity at the surface.

Another study that suggested a connection between IN and biological activity in the ocean was reported by *Schnell* [1977]. During a cruise off the coast of Nova Scotia (41°-45°N) he obtained filter samples of aerosol particles and estimated IN concentrations of 0.001 to 0.5 L^{-1} at -15°C. Drop-freezing studies were done on seawater samples; they froze as warm as -4°C. The highest concentration of IN were associated with regions having the greatest biological content of seawater (glycoprotein), leading to the suggestion that IN activation may be related to bacteria in the seawater. A more comprehensive review of this topic can be found in the work of *Szyrmer and Zawadzki* [1997].

1.3. Chemical Composition of Ice Nuclei

Ice nuclei are a special subset of the total aerosol, characterized only by their ability to nucleate the ice phase. Measurements of IN are difficult because the activity of IN depends on both temperature and humidity, there are multiple nucleation mechanisms, and there is no clear association with size or chemical properties of the IN particle.

There are very few studies of the chemical composition of single IN particles. *Kumai* [1976] and *Kikuchi et al.* [1982] collected falling snow crystals and examined particles at the geometric centers using an electron microscope. The particles were clay minerals and sodium chloride, suggesting marine and terrestrial origins. In both of these studies, the crystals were large (100 - 1000 μm), aged (hundreds of seconds), and fell a substantial distance as they grew. The technique has uncertainty that a residual particle is the ice-nucleating particle since other particles could be collected by scavenging [e.g., *Murakami et al.,* 1985]. The technique we used for collecting IN minimizes the likelihood of this uncertainty because the crystals nucleate and grow within the CFD chamber and are collected within < 10 s of nucleation; there is insufficient time for any process besides nucleation to attach other particles to the crystal [*Kreidenweis et al.*, 1998]. Evidence from other studies has suggested that there may be distinguishing chemical differences between the IN and non-IN aerosol populations and between natural aerosol particles and those affected by pollution [e.g., *Borys*, 1986; *Rosinski et al.*, 1987; *Chen et al.*, 1998]. *Chen et al.* [1998] presented transmission electron microscope (TEM) analyses of upper tropospheric particles indicating that the elemental composition of ice nuclei was systematically different from the total ambient aerosol: the IN samples had consistently greater metallic, crustal and carbonaceous fractions and a much smaller fraction of sulfate.

1.4. FIRE ACE and SHEBA Projects

The goals of the research described here are to estimate the concentrations, activity, spatial distributions, sizes, and chemical composition of IN aerosols in the Arctic. In 1998 there were two overlapping field experiments in the Arctic Ocean, the NASA FIRE Arctic Cloud Experiment and SHEBA (Surface Heat Budget of the Arctic). Several research aircraft were involved, including the NCAR C-130 that was based out of Fort Wainwright near Fairbanks, Alaska. Airborne measurements of IN were made on eight flights of the NCAR C-130 aircraft during May 1998. This paper describes those measurements, shows examples of the data from one flight, and gives general summaries of the results. For information about other studies that were part of these projects, the reader is referred to companion papers in this special issue.

2. Description of Equipment and Sampling Procedures

2.1. Instrumentation

The primary measurements in this study include ice nuclei, condensation nuclei (CN), cloud particles, atmospheric state parameters, and winds. The IN and CN instruments shared a common sample inlet, as shown in Figure 1. This inlet piping was continuously flushed with a large flow of ambient air (~1000 L min^{-1}); residence time through the main piping was < 0.5 s. At the Colorado State University (CSU) instrument rack, small flows were divided between the CFD (~1 L min^{-1}) and the CN counter (~1.5 L min^{-1}). During selected periods of ~30 min, additional aerosol particle samples were collected on membrane filters. Other samples were taken by using a PIXE® impactor to collect particles onto electron microscope (EM) grids.

Ice nuclei were measured with CSU's continuous flow diffusion (CFD) chamber [*Rogers et al.*, 2001]. The CFD is a thermal gradient diffusion chamber of concentric cylinder design [*Rogers,* 1988, 1994]. In this chamber, air flows in the vapor supersaturated space between two ice-coated cylinders that are at different temperatures. The sample air occupies the central 10% of the flow and is sandwiched between particle-free sheath flows; that is, the total volume flow is ~10 L min^{-1}, and the sample flow is ~1 L min^{-1}. Active IN aerosols form ice crystals that grow in the chamber to ~3 μm diameter or larger, depending on temperature, humidity, and residence time, and these crystals are detected at the chamber outlet. This technique is sensitive to deposition and condensation-freezing nucleation processes. As operated during this project, the CFD was not sensitive to contact-freezing or homogeneous freezing (a laboratory version of the chamber is capable of homogeneous-freezing measurements). Particles >3 μm (ice crystals) are counted at the chamber outlet by an optical particle counter (OPC). Typical residence time was 3-5 s.

An inertial impactor was located immediately downstream of the OPC in order to capture crystals (containing IN) on TEM grids during selected time periods. The IN impactor samples were accumulated over 20 to 60 min intervals in order to collect several hundred particles. The impaction substrate is a copper TEM grid with Formvar backing and a thin carbon coating. Samples from the crystal impactor and the PIXE® impactor were analyzed at CSU and RJ Lee Associates using transmission electron microscopy and energy dispersive X-ray (EDX) microprobe techniques to determine the number, size, and physicochemical characteristics of single particles [*Kreidenweis et al.,* 1998; *Chen et al.,* 1998]. The minimum particle size for EDX analysis is ~0.1 μm, but the size limit is affected by detector sensitivity, atomic number, and mixed composition of particles [*Markowitz et al.,* 1986]. The size limit of 0.1 μm is within the range ex-

pected for IN particles [e.g., *Rosinski et al.,* 1987; *Chen et al.*, 1998].

Studies by *Okazaki and Willeke* [1987], *Huebert et al.* [1990], *Porter et al.* [1992] indicate that the sampling and transmission characteristics of air inlets and associated piping can strongly affect aerosol measurements from aircraft. The inlet system used in this study caused diffusion losses in the smaller piping, air deceleration heating, and choking off the airflow when rime ice briefly formed over the inlet in supercooled water clouds. The flow rate was adjusted to obtain isokinetic sampling, avoiding a size bias from this effect. We also deliberately added a size cut to the sampled aerosol stream with an impactor at the upstream end of the CFD chamber. It removed particles >2 μm, so that they were not inadvertently classified as ice crystals by the optical counter at the CFD outlet.

Particle losses occur in the inlet tubing, tees and valves due to diffusion and inertial deposition. The correction for these losses depends on the particle size distribution, humidity, particle volatility, electrical charge, flow rate, temperature, and pressure. We estimated this loss empirically with the CN counter by sampling cabin air with and without the piping. The resulting correction factor was 1.4, based on several tests before and during the field project. The greatest diffusion losses occur for particles 0.010 to 0.1 μm. Laboratory measurements (840 mb) of our sampling system showed the diffusion losses were ~20% for particles 0.07 to 0.2 μm, increasing to 50% at ~0.025 μm. Corrections were applied to the CN data, based on empirical estimates obtained in the field. For IN ice-nucleating particles, no information is available on their size or other factors upstream of sampling, and no corrections were applied.

Travel times to the CN counter and through the CFD chamber were estimated by alternately sampling cabin air or particle-free air at the point where samples were taken from the large flow piping. The response time was 5 s, and this correction was applied to IN and CN data.

On several occasions in supercooled liquid water clouds (-5° to -12°C and > ~0.1 g m^{-3}), there was evidence that the air sample flow was affected by rime ice obstructing the inlet. When the aircraft flew out of cloud, the ice melted or broke off, and the sample flow was restored within ~30 s. As long as the aircraft remained in supercooled water cloud, the sample airflow decreased progressively. When the C-130 flew through clouds, ice crystals and cloud drops were drawn into the sample tube along with the air. It is likely that some droplets and crystals impacted on the walls of the tube; some of these may have broken into fragments and rebounded while others stuck. Drops and crystals would also evaporate as the sample air decelerated on entering the tube, warming and drying by compressional heating; the residual particles of evaporated crystals could pass on to the aerosol instruments. The effect of cloud particle residues on IN and CN measurements is unknown. We made no evaluation of or accounting for such effects. All in-cloud periods were included in our analyses.

Measurements of CN concentration were made with butanol-type instruments (TSI 3076). Laboratory studies by *Wiedensohler et al.* [1997] showed that CN detection sensitivity decreases with particle size below ~0.020 μm diameter, with 50% detection at ~0.010 μm. There were three independent CN instruments on the C-130 aircraft, sampling from as many as three different inlets (Figure 1).

Several different instruments on the C-130 detected cloud drops and precipitation-size particles (ice crystals or drizzle drops). Estimates of ice crystal concentrations were made from PMS 2D-C and 1D (260-x) probes; cloud droplets were detected with PMS (Particle Measuring Systems, Inc.) FSSP-100 and FSSP-300 probes, and liquid water content came from the PMS King hot wire device.

2.2. Sampling

The focus of these flights was the SHEBA ice camp, an extensively instrumented surface site based at the ice breaker ship *Des Groseilliers*. By May 15, 1998, the ship had drifted 8 months with the Arctic Ocean pack ice and was ~500 km northwest of Barrow, Alaska, or ~1400 km northwest of Fairbanks. The ferry flight from Fairbanks to the ice camp took about 2.5 hours. Once on station near the ice camp, the C-130 usually flew a raster-type track at high altitude (4 km) for an hour and then descended to lower altitudes for additional mapping of surface features and cloud penetrations. Measurements of aerosol particles occurred throughout the flights.

The CFD measures ice nuclei activity at one set of temperature and supersaturation (T,SS) conditions at a time. Different conditions are obtained by changing temperatures of the chamber walls, and a few minutes are needed to stabilize at the new conditions. Our sampling strategy was to attempt using a range of sampling conditions that overlapped local clouds and cloud-forming regions. The Arctic winter-spring transition occurred during these May flights, ultimately producing low-altitude temperatures too warm for our chamber, -5° to 0°C; therefore measurements were made at colder temperatures.

Over a period of time, samples were taken both above and below water saturation, with the maximum supersaturation typically about +5% and the minimum typically -10%. The general strategy was to maintain constant (T,SS) conditions during vertical profiles and when impactor samples were collected. Conditions were varied to obtain a (T,SS) spectrum when flying at constant altitude in a relatively homogeneous region, for example during ferry flights between Fairbanks and the SHEBA ice camp. Occasionally, samples were made at very high SS_w (>10%) for a few minutes.

Counts of IN (crystals) were measured at 10 Hz and then averaged to 10 s to increase the number of nonzero values while still preserving some of temporal resolution. Since the C-130 typically flies at ~100 m s^{-1}, the 10 s IN averages correspond to ~1 km. The other data (CN, temperature, cloud particles) are based on 1 Hz data.

2.3. Range of Measurements

As shown in Figure 2, IN measurements were made over wide ranges of temperature and supersaturation during the eight flights in May: from -10° to -34°C and from ice saturation to 20% supersaturation with respect to water. Although measurements were made throughout these long flights (~10 hours each), the data were reduced for the analyses in this paper to include only those (1) when simultaneous CFD and aircraft data were available, (2) within a 100 km box centered on the SHEBA ship, and (3) with CFD water supersaturations ≤ 5%. Not included in the statistical summaries are a small number of measurements with higher SS_w (up to +20%). They are excluded because such large supersaturations are not representative of typical conditions in Arctic clouds, and the calibration and interpretation of the CFD technique for such high supersaturations is still an object of study. These three criteria reduced the amount of data to ~40% of the total obtained.

The range of measurements varies from one flight to the next, with considerable overlap, as shown in Figure 2. For the IN data

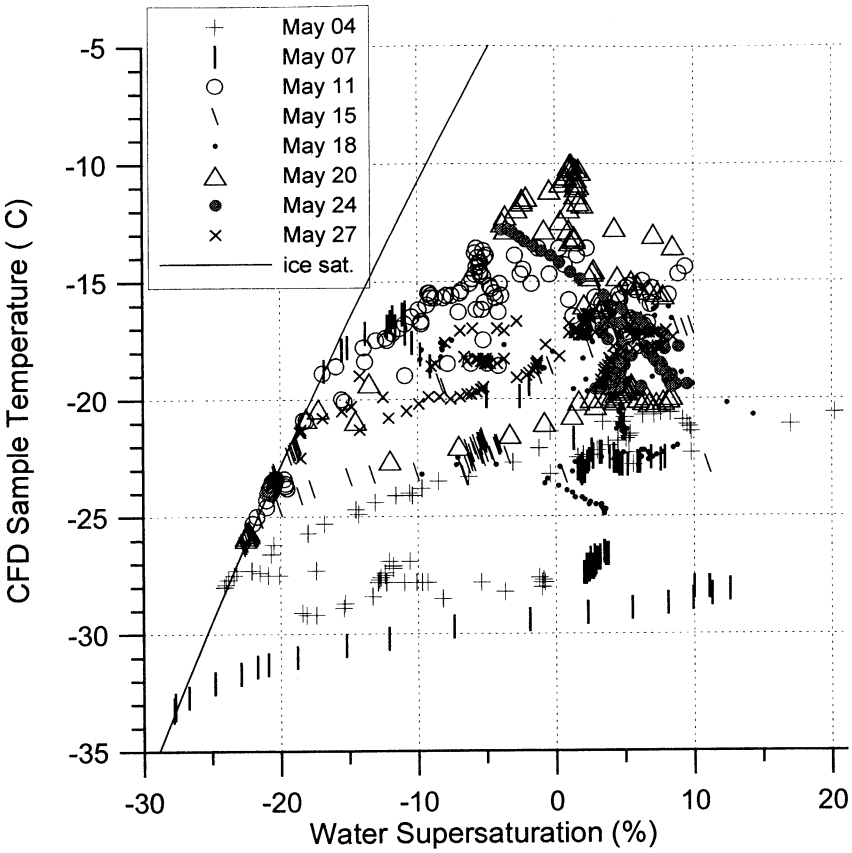

Figure 2. Range of ice nuclei sampling conditions for CFD chamber while aircraft was within 100 km of Surface Heat Budget of the Arctic (SHEBA) ship during eight flights. Each point represents 1 min or ~1 L. Total, 941 points.

in this analysis, 49.6% of the measurements were made with CFD sampling conditions below water saturation.

3. Examples of Measurements

Examples of ice nuclei measurements and aircraft data are shown in Figures 3 and 4 for several hours of the May 15 flight when the C-130 was within 100 km of the SHEBA ship. Vertical pointing radar at the ship showed that a thin stratus cloud with a top of ~1.8 km was present and precipitating until 1800 UTC, three hours before the aircraft arrived. At about the time this cloud dissipated and disappeared from radar, a very thin low-level stratus cloud was present and persisted throughout the remainder of the flight. Radar, lidar, and aircraft measurements indicated that the low-level cloud consisted primarily of supercooled water.

Calculations of air mass trajectories indicated that air from the surface to 1.5 km came from the southeast, across a large region of the Arctic ice pack. At 3 km, trajectories were southerly, bringing air from Alaska. Above that, the trajectories were westerly.

3.1. Vertical Profile

After arriving over the ship, the C-130 descended from 6.5 km to 4.0 km where it spent ~45 min collecting surface imagery of the pack ice; then it descended to the surface. Figure 3 shows some of the aircraft and ice nuclei measurements during the descent from 4 km to the surface. The strong vertical structure is revealed in the temperature, humidity, cloud particle, and aerosol measurements. There were three strong stable layers, at ~1500, 700, and 400 m. Above 1330 m the atmospheric humidity was less than ice saturation. The higher humidity layer from 1100 to 1300 m may have been a residual from the earlier cloud. The 260-x probe detected a very thin remnant of cloud particles at 2.6 km with concentrations up to 140 L^{-1}; these particles were ~60 to 100 μm in size with a few to 160 μm. The low-level cloud was found in two thin layers, 120-300 m and 600-650 m, and was -8° to -10°C. The 2D-C probe detected ice or water particles in concentrations zero to 0.4 L^{-1} (based on the shadow-OR signal). The greatest liquid water content was 0.2 g m^{-3} near the top of the lower cloud.

While the aircraft was at 4 km, IN and ambient particle collections were taken for single-particle analysis. During the descent, IN measurements were made at –5 to -7% SS_w and -22°C (13°C colder than the low-level cloud). The average IN concentration was ~16 L^{-1}, with a peak of 70 L^{-1} near the surface. The aircraft then descended through the multiple inversions and the low-level cloud, and spent the next hour flying transects near SHEBA at altitudes from ~30 m to ~700 m above ground level (AGL).

Above 500 m, background CN concentrations were ~300 to 1000 cm^{-3} at standard temperature and pressure (STP). There were occasional brief spikes of much higher CN when the airplane crossed its own exhaust. The smallest CN values were seen in the surface layer, as small as ~20 cm^{-3}. Although the traces of Passive Cavity Aerosol Spectrometer Probe (PCASP, 0.3 - 3 μm) and CN usually tracked together, there were instances when they were anticorrelated. Examples for both trends can be seen in Figure 3 during the descent, for example at ~1.8 and 2.8 km. The

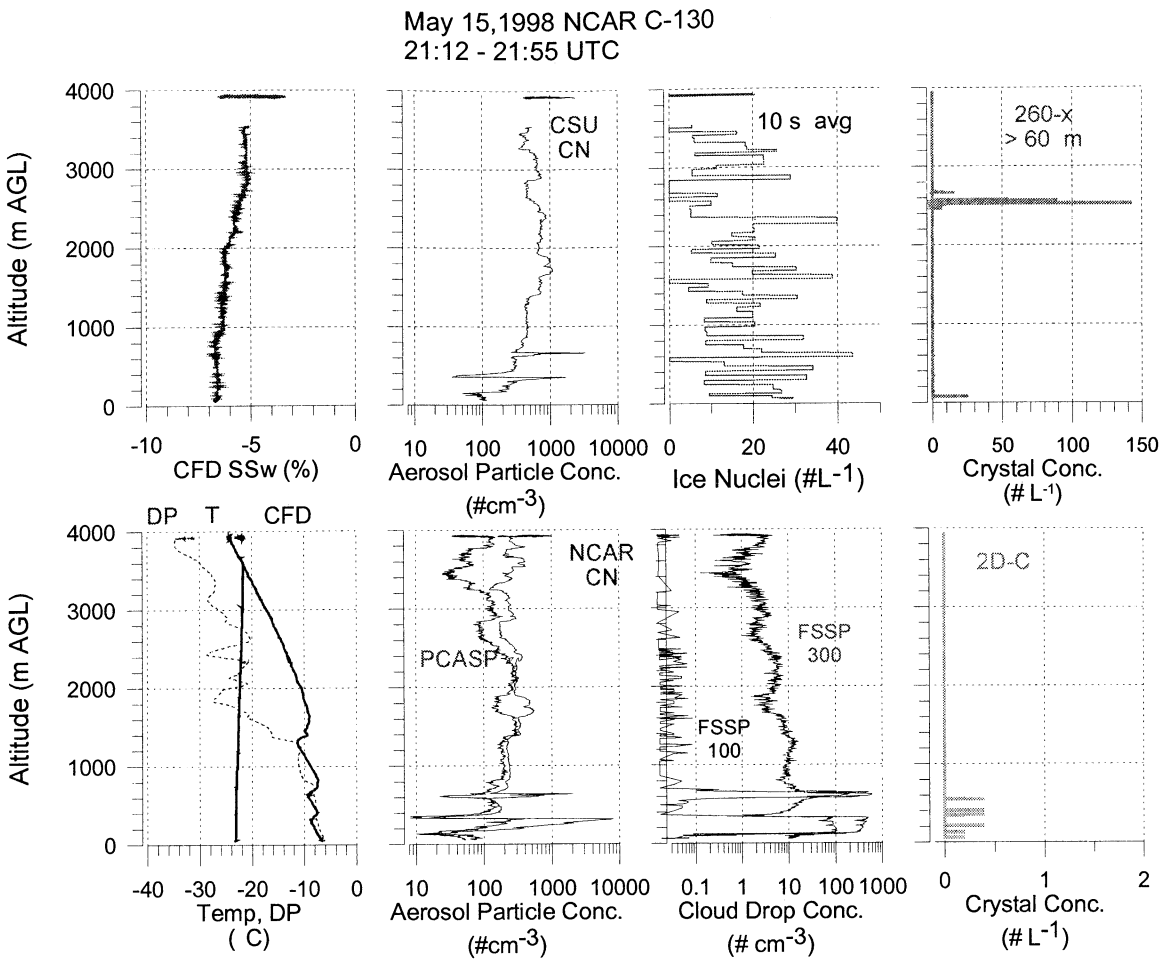

Figure 3. Vertical profile of aircraft and ice nuclei measurements during descent near SHEBA ice camp. IN and Colorado State University (CSU) CN number concentration per unit volume at standard temperature and pressure (STP). All other concentrations use ambient volumes. Two independent CN counters were available.

recent existence of cloud at ~1.8 km suggests that scavenging and coagulation might explain the lower PCASP numbers. It has been suggested [*Hegg et al.,* 1991] that the tops of stratiform clouds are favored regions for the formation of new CN and that may be an explanation in this case. Enhanced CN inside the cloud (700 m and 200 m) may be an artifact of particles produced by cloud water splashing on the air sample inlet.

3.2. Low-Level Transects

An hour later, the aircraft was performing transects of the surface layer and low-level cloud near the SHEBA ship. Figure 4 shows the history of data during this time. Initially, the aircraft was ~40 km north west of the ship flying very low (~30 m) over open water leads. Radiometric surface temperatures were ~4°C higher over open water leads than over ice (Figure 4, bottom panel). From 2312 to 2328, IN measurements were made at -15° to -19°C, and SS_w was varied from 2 to 10% with little effect on IN concentration. The IN average was 9.8 L^{-1} with a maximum of 41.

There are two prominent IN features: the abrupt increases to ~100 L^{-1} at 2346 and 2352. Both of these peaks occurred when the aircraft was at slightly higher altitude during turns; the latter peak may be associated with cloud penetration as the aircraft ascended. With southeasterly air flow in the surface layer, the aircraft was upwind of the SHEBA ship when the high IN features were encountered, hence the ship was not the source of these narrow regions of high IN. As mentioned earlier, there is historical evidence that sea water is a source of IN [*Schnell* 1977; *Rosinski et al.*, 1986, 1987]. Perhaps the peaks of IN that were observed in this flight have their sources in open water leads in the pack ice. The presence of leads is suggested by radiometric temperatures ~-3°C (Figure 4, bottom) and visual observations from the aircraft. We have no convincing evidence of a connection between our IN measurements and leads, but we mention it as an interesting possibility.

Figure 4 shows precipitation-size particles (ice crystals or drizzle drops) were detected 2331-2341 by the 2D-C probe (dots, up to 78 L^{-1}, geometric mean 1.6 L^{-1}) and 260-x probe (up to 879 L^{-1}, geometric mean 20 L^{-1}). Observer notes and images from the SPEC CPI probe indicate these were mostly drizzle drops, not ice crystals, and they were 50-200 μm diameter according to the 260-x. It is noteworthy that drizzle was produced by this long lived cloud that was only 200 m thick.

Prominent CN features are the spikes at 2316, 2318 and 2343, when the airplane crossed its own exhaust. Note that the exhaust produced no effect on IN. After 2330 the aircraft was in a region with very low CN concentrations, 20-30 cm^{-3}, as indicated on two CN instruments. By the end of this time period, the aircraft

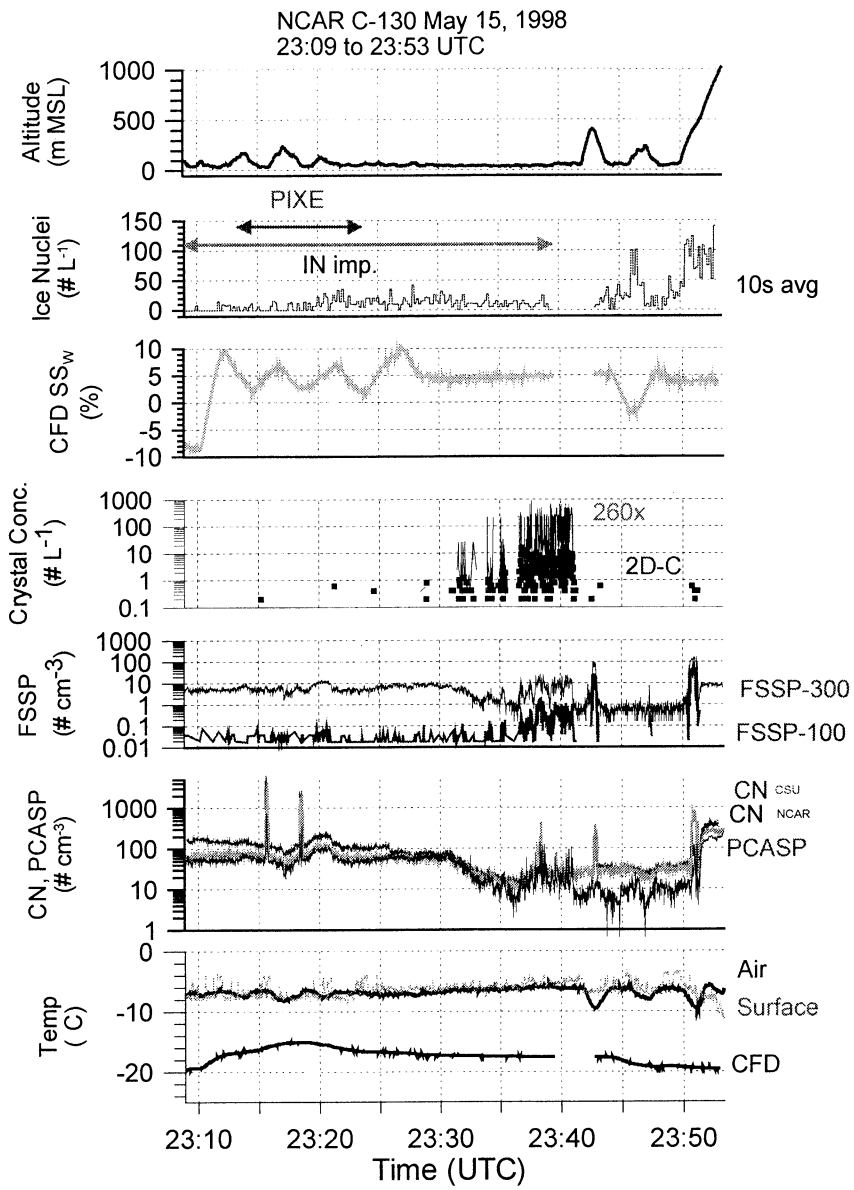

Figure 4. Time history of 45 min of aircraft and ice nuclei measurements near SHEBA ice camp at low altitudes. IN data gaps occur when particle samplers were changed (PIXE and IN imp). Note periods of remarkably low CN concentration (30 cm^{-3}) and small regions with higher IN concentrations (2346 and 2351). Warmer surface temperatures (bottom) show open water leads. (panel 4) Ice crystals or drizzle drops 2D-C (dots) and 260-x probes.

was ~40 km southeast of the ship where there were more open water leads. At 2350 the C-130 ascended through the thin cloud.

3.3. Single-Particle Analyses

Samples of IN and ambient particles were collected on the May 15 flight (labeled PIXE and IN imp. in Figure 4), and the results of EM analyses are summarized in Table 1. The reader may recall that potential IN larger than 2 μm are removed by the impactor upstream of the CFD instrument, hence we have no measurements of IN > 2 μm. The EM analysts were asked to give a characteristic size and shape for each particle. As mentioned earlier, the minimum for particle sizing and EDX analysis is ~0.1 μm. For circular images (spherical particles) the size is the diameter, and for non-circular images it is the average of the maximum and perpendicular dimensions. Table 1 shows that the average size of IN particles collected on the crystal impactor was 0.52 μm, slightly larger than the average of all particles. The morphology and composition of IN varied widely. For a circular particle the shape was assigned the value 0; for noncircular particles the shape was 1. Table 1 shows that the average shape of the "all-particle" collection was spherical, but for IN it was 0.85.

Elements detected in the ice nuclei samples included Si and metals (Al, Ca and Zn). The majority of IN particles (76%) had weak or no X-ray signatures. These particles were imaged but indicated no detectable element. Minimum limits for detection by the X-ray microprobe technique derive from elemental mass, electron cross section and transmittance of the detector window. emissions from elements lighter than approximately sodium (Z=23) were not detectable by the equipment we used. Hence there are several possible compositions for those particles having no X-ray signature. We suspect they are probably carbonaceous because of their appearance (morphology) and stable behavior of

Table 1. Summary of Electron Microscope Analysis for Particles ~0.1 to 2 μm, Ice Nuclei and All Particles from May 15 Flight[a]

		Size	Shape 0 Sphere	Percent															No
	Particles	(μm)	1 Other	Al	Ca	Cl	Co	Cr	Fe	K	Mg	Na	S	Sb	Si	Sn	Ti	V	Zn	X-Ray
Ice nuclei	42	0.52	0.85	2	2	0	0	0	0	0	0	0	0	0	14	0	0	0	5	76
All particles	40	0.35	0.00	0	0	0	0	0	0	0	0	0	95	0	5	0	0	0	0	0

Percent of particles containing indicated element (rounded to nearest whole percent).

the particles when exposed to the electron beam in the microscope's high vacuum environment. In contrast to the IN, particles in the *total* aerosol sample contained a high proportion of sulfur, and all of them produced X-ray signatures. Other elements were listed but show zero percent occurrence in Table 1. These elements were detected in one or more particles in other samples and are shown for consistency with Table 3, which summarizes a larger data set.

4. Mean IN Properties

4.1. Average Vertical Profiles of IN

The IN measurements from all eight flights were stratified according to water supersaturation of the measurements in order to separate different nucleation modes. Below water saturation ($SS_w < 0$) the measurements represent deposition (sorption) nucleation. Above water saturation ($0 \leq SS_w \leq 5\%$) they represent the sum of deposition and condensation-freezing modes.

The Arctic atmosphere typically shows stable thermodynamic stratification, with distinct layering of aerosol particle concentrations, as illustrated in the May 15 case. Thermodynamic soundings at the SHEBA ship were examined to help select altitudes where stable layers were often present. We stratified the IN data into four different altitude layers: surface to 500 m, 500 to 1000 m, 1000 to 3000 m, and everything above 3000 m. These layers contain 39, 15, 18 and 28%, respectively, of the data summarized here.

The results are shown in Table 2 for each of the flights. The entries are arranged according to altitude as an aid to interpretation. Notice that on any one day, the sampling temperatures were generally constant, as planned, although there are exceptions. These are not true vertical profiles, since the aircraft usually

Table 2. Ice Nuclei Concentrations (Number per STP Liter) Near SHEBA Ship During 1998 Flights

	May 4		May 7		May 11		May 15	
Altitude	$SS_w < 0$	$0 \leq SS_w \leq 5\%$	$SS_w < 0$	$0 \leq SS_w \leq 5\%$	$SS_w < 0$	$0 \leq SS_w \leq 5\%$	$SS_w < 0$	$0 \leq SS_w \leq 5\%$
> 3000 m	X	X	0-18 (0.71) –32°C	0-9.2 (0.5) –27°C	0-73 (4.8) –21°C	0-54 (12) –15°C	0-26 (2.7) –23°C	X
1000 to 3000 m	0-75 (19) –28°C	29 (29) –27°C	X	0 (0) –27°C	0-40 (4.3) –17°C	0-11 (0.54) –16°C	0-40 (6.7) –22°C	X
500 to 1000 m	0-65 (18) –28°C	X	X	0-65 (1.7) –27°C	0-46 (5.5) –15°C	0-0.27 (0.15) –17°C	0-43 (17) –23°C	51-141 (88) –20°C
Surface to 500 m	0-43 (2.6) –26°C	0-73 (1.8) –22°C	0-40 (4.4) –18°C	0-1645 (57) –25°C	0-107 (7.2) –16°C	0-5.4 (2.6) –17°C	0-101 (25) –21°C	0-124 (17) –17°C

	May 18	May 18	May 20	May 20	May 24	May 24	May 27	May 27
> 3000 m	0-93 (19) –21°C	0-104 (16) –21°C	0-37 (3.6) –24°C	0-73 (19) –20°C	0-97 (24) –24°C	0-60 (10) –18°C	0-66 (9.8) –20°C	0-381 (17) –17°C
1000 to 3000 m	X	0-19 (4.7) –19°C	0-24 (2.4) –14°C	0-117 (2.5) –11°C	0-38 (4.5) –13°C	0-34 (5.7) –17°C	0-31 (4.7) –18°C	0-19 (3.5) –17°C
500 to 1000 m	0-6.8 (0.48) –18°C	0-13 (1.4) –19°C	X	0-7.1 (1.2) –10°C	X	0-28 (4.2) –19°C	0-8.7 (1.2) –21°C	0-32 (7.5) –19°C
Surface to 500 m	0-6.8 (0.08) –21°C	0-62 (4.6) –22°C	X	0-58 (8.1) –13°C	X	X	0-23 (4.4) –19°C	0-292 (9.5) –17°C

Values are based on 10 s averages and are organized by altitude ranges and sub-saturation or super-saturation with respect to water. min-max (average) sampling temperature; X indicates no data.

Table 3. Similar to Table 1 But for Five Flights (May 4, 11, 15, 20 and 24) and Differentiated by Altitude of Collection High (700-3000 m) or Low (50-170 m)

		Size	Shape 0 Sphere	Percent															No
	Particles	(μm)	1 Other	Al	Ca	Cl	Co	Cr	Fe	K	Mg	Na	S	Sb	Si	Sn	Ti	V	Zn	X-Ray
IN high	110	0.46	0.82	3	2	0	0	0	2	2	0	2	7	0	38	1	0	0	5	38
IN low	152	0.36	0.68	1	2	0	0	1	5	0	1	15	18	0	37	0	2	0	0	14
AP high	80	0.41	0.06	1	0	0	0	0	1	2	1	1	87	0	6	0	0	0	0	1
AP low	123	0.50	0.04	1	1	0	0	1	1	3	1	3	59	0	29	2	0	0	0	2

stayed at one altitude for tens of minutes and then changed altitude along a slantwise path. Also, the subsaturated sampling could be several hours and many kilometers apart from the supersaturated sampling.

Several features that show up in the table include the following:

1. Minimum IN concentrations were always zero; or more correctly, the minimum IN < 0.16 L^{-1}, since the 10 s sample volumes were ~1/6 L.
2. Distributions were always positively skewed (mean values were always closer to the minimum).
3. The occurrence of substantial IN concentrations occurring below water saturation is surprising. We expected that IN concentrations measured above water saturation would exceed those below water saturation, if sampling temperatures were nearly the same and atmospheric conditions were relatively uniform. However, this expectation is not borne out in the average values of Table 2. It was seen in shorter periods of sampling, when the aircraft was in regions having relatively homogeneous composition.
4. Very rarely, extremely high concentrations were seen in the surface layer for water supersaturation (e.g., the May 7 maximum of 1645 L^{-1}). These occurrences were always of very short duration (~20 s).

4.2. Fraction of All Particles Active as IN

The fraction of all particles active as IN can be estimated as the ratio of IN and CN concentrations. Figure 5 shows this ratio along with other cumulative probability distributions of the ice nuclei and CN measurements for all eight flights, when the aircraft was within 100 km of the ice camp. This overall summary figure shows that the IN/CN ratio varied from zero to ~0.02, with

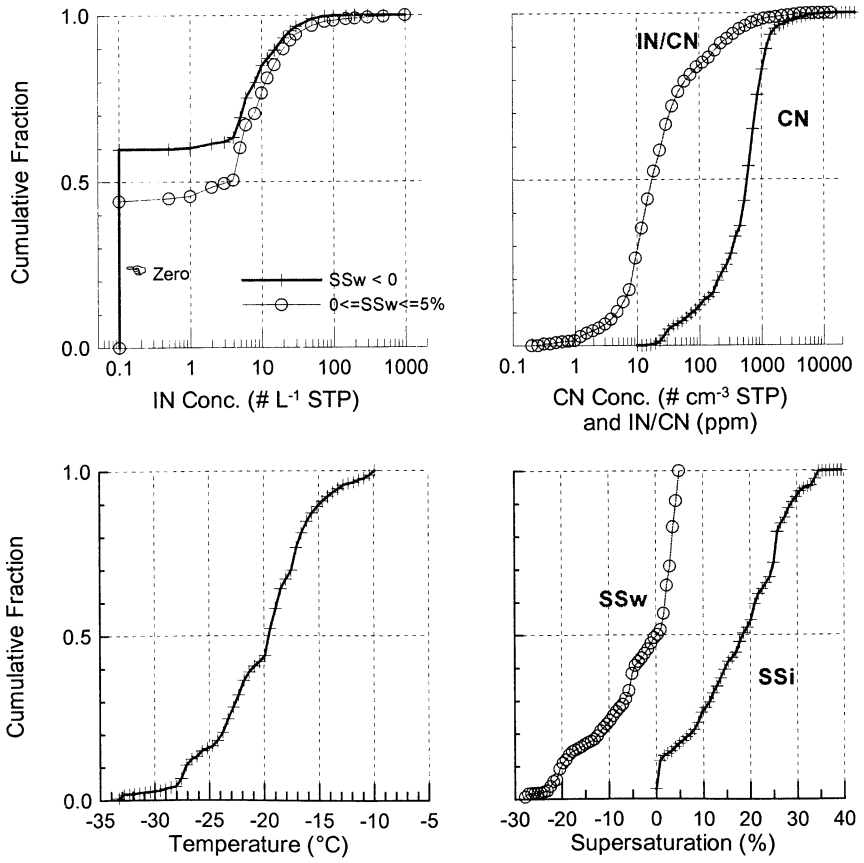

Figure 5. Cumulative frequency distributions of 10 s average ice nuclei and CN concentrations and CFD chamber sampling conditions for eight flights in May 1998. For plotting convenience on logarithmic scale, zero IN concentration was plotted at 0.1. Total number of points, 41196.

a median ~20 ice nuclei per million CN. Median CN was ~600 cm^{-3}, and values associated with extremely clean air (<100 cm^{-3}) occurred ~10% of the time.

Because the IN concentrations covered a very wide range the probability distribution was calculated using geometrically increasing bins of concentration. The IN curves are unusual because they are so highly skewed. Concentrations of zero IN comprised ~60% of the 10 s measurements below water saturation, and ~45% of those above water saturation. Notice that on average, higher SS_w was associated with greater IN concentrations, as expected. Nevertheless, some very high concentrations were measured below water saturation.

4.3. Summary of Single-Particle Analyses

Collections of all particles (AP) and IN were analyzed from five Arctic flights (May 4, 11, 15, 20, and 24), and the results are summarized in Table 3. These analyses are limited to particles ~0.1 to 2 μm. Trends that were seen in the May 15 case (Table 1) are evident in this larger data set. IN particles were a few tenths micrometer in size and nonspherical, in contrast with the AP samples which were more often spherical. The dominant elements detected in the IN samples included Si, S, and some metals (Zn, Al, Fe). S and Na were more common for low- altitude IN. Significant fractions of the particles exhibited weak or no X-ray signatures, due to small mass or low atomic numbers (e.g., elemental or organic carbon). In contrast, a high proportion of AP contained primarily S, or Si and S, and only a few (1-2%) exhibited no X-ray signature. These results are in general agreement with *Chen et al.* [1998] who reported that the elemental compositions of IN are systematically different from the total ambient aerosol.

5. Discussion

Aerosol particle concentrations in the late winter/early spring Arctic atmosphere had typical CN concentrations of a few hundred cm^{-3} over extended regions and occasionally as low as ~20 cm^{-3}. These values are generally consistent with earlier airborne Arctic aerosol studies. For example, *Barrie* [1986] reported CN 10 to 4000 cm^{-3}, with geometric mean 200-350 cm^{-3}. *Brock et al.* [1989] had typical background CN ~200 cm^{-3} (STP) with peak values 3100 cm^{-3}. *Borys* [1989] had 25 to 5000 cm^{-3} over large transects of the Arctic, and *Herbert et al.* [1989] found CN minima of 100 cm^{-3} and maxima of 8000 cm^{-3}. We suspect that the lowest values were associated with air that underwent several cycles of cloud-scavenging processes and was far removed from anthropogenic influence.

Our IN measurements covered a wide range of temperatures and humidities, -34° to -10°C and from ice saturation to 20% water supersaturation (Figures 2 and 5). Even with restricting the maximum SS_w to 5%, the range of IN concentrations was very large. Not including the zeroes, it covered 5 orders of magnitude. The low end of IN concentration was generally consistent with earlier Arctic IN measurements that used membrane filter methods and averaged over tens of minutes. The median and high end of our data are much larger than earlier measurements.

Cloud microphysical evidence of the paucity of IN was found in thin low-level stratus clouds at -15° to –20°C. These clouds had low concentrations of ice crystals (~1 L^{-1}), a few tenths g m^{-3} of supercooled liquid water and persisted for several days. We estimated the frequency of occurrence of such clouds for the month of May 1998 by examining 10 min average time-height histories of remote sensing data from the SHEBA ice camp (NOAA Environmental Technology Laboratory 35 GHz radar and depolarization and backscatter lidar). Descriptions and examples of the remote sensing observations are in the work of *Curry et al.* [2000]. The analyses indicate that low-level stratus clouds were detected 48% of the time during May, i.e., when the lidar was attenuated below 1 km altitude and the radar echo showed that a top of the stratus cloud was below 1 km. Other aspects of the low-level stratus clouds are described in several of the companion papers in this issue, including *Hobbs et al.* [2001], *Shupe et al.* [this issue] and *Minnis et al.* [this issue].

Although strong vertical stratifications were often seen in aerosol concentrations at inversion layers, strong stratifications were not noticed for IN, except that the only place where small regions of high IN concentrations were seen was at low altitudes (~100 m) over the pack ice. This was an unexpected and surprising observation. The small area in which high IN were observed suggests that the source may be nearby (perhaps of biological origin from open water leads) or that higher IN concentrations might be confined within thin stable layers.

Single-particle EM analyses indicate that IN particles are generally a few tenths micrometer in size, with morphology and composition varying widely. Elements detected in ice nuclei include Si, S, and some metals (Zn, Cr, Al). When examined with EDX, many IN particles produced weak or no X-ray signatures, most likely due to the dominance of a low-molecular-weight component not detected by the EDX system; this component is probably carbon. This observation differs from the total aerosol samples, for which most particles (>98%) produced an X-ray signature.

Acknowledgments. This material is based on work supported by NASA grants NAG-2-924 and NAG-1-2063, and National Science Foundation grants ATM-9311606 and ATM97-14177. Any opinions, findings, and conclusions or recommendations expressed in this material are those of the authors and do not necessarily reflect the views of the National Science Foundation. We wish to acknowledge the technical support from the Research Aviation Facility at NCAR for helping us install the instruments and conduct the flights. We are grateful for the dedicated work of other FIRE – ACE and SHEBA investigators whose observations are helping our studies.

References

Albrecht, B.A., Aerosols, cloud microphysics, and fractional cloudiness, *Science, 245,* 1227-1230, 1989.

Baker, M.B., Cloud microphysics and climate, *Science, 276,* 1072-1078, 1997.

Barrie, L.A., Arctic air polution: An overview of current knowledge, *Atmos. Environ., 20,* 643-663, 1986.

Bigg, E.K., Ice nucleus concentrations in remote areas, *J. Atmos. Sci., 30,* 1153-1157, 1973.

Bigg, E.K., Ice forming nuclei in the high Arctic, *Tellus, 48 Ser. B,* 223-233, 1996.

Bigg, E.K., and C.M. Stevenson, Comparison of concentrations of ice nuclei in different parts of the world, *J. Rech. Atmos., 2,* 41-58, 1970.

Borys, R.D., Studies of ice nucleation by Arctic aerosol on AGASP-II, *J. Atmos. Chem., 9,* 169-185, 1989.

Brock, C.A., L.F. Radke, J.H. Lyons, and P.V. Hobbs, Arctic hazes in summer over Greenland and the North American Arctic, I, Incidence and origins, *J. Atmos. Chem., 9,* 129-148, 1989.

Chen, Y., S.M. Kreidenweis, L.M. McInnes, D.C. Rogers, and P.J. DeMott, Single particle analyses of ice nucleating particles in the upper troposphere and lower stratosphere, *Geophys. Res. Lett., 25,* 1391-1394, 1998.

Chen, Y., P.J. DeMott, S.M. Kreidenweis, D.C. Rogers, and D.E. Sherman, Ice formation by sulfate and sulfuric acid aerosol particles under upper-tropospheric conditions, *J. Atmos. Sci., 57,* 3752-3766, 2000.

Cooper, W.A., Ice initiation in natural clouds. in Precipitation enhancement — a scientific challenge, in *Meteorological Monogr., vol. 21,* pp. 29-32, Am. Meteorol. Soc., Boston, Mass., 1986.

Curry, J.A., F.G. Meyer, L.F. Radke, C.A. Brock, and E.E. Ebert, Occurrence and characteristics of lower tropospheric ice crystals in the Arctic, *Intl. J. Clim., 10,* 749-764, 1990.

Curry, J.A., W.B. Rossow, D. Randall, and J.L. Schramm, Overview of Arctic cloud and radiation characteristics. *J. Clim., 9,* 1731-1764, 1996.

Curry, J.A., et al., FIRE Arctic Clouds Experiment, *Bull. Am. Meteorol. Soc., 81,* 5-29, 2000.

Fountain, A.G. and T. Ohtake, Concentrations and source areas of ice nuclei in the Alaskan atmosphere, *J. Clim. Appl. Meteorol., 24,* 377-382, 1985.

Fowler, L.D., and D.A. Randall, Liquid and ice cloud microphysics in the CSU General Circulation Model, part II, Impact on cloudiness, the earth's radiation budget, and the general circulation of the atmosphere, *J. Clim., 19,* 530-560, 1996.

Hegg, D.A., L.F. Radke, and P.V. Hobbs, Measurement of Aitken nuclei and cloud condensation nuclei in the marine atmosphere and their relation to the DMS-cloud-climate hypothesis, *J. Geophys. Res., 96,* 18,727-18,733, 1991.

Herbert, G.A., R.C. Schnell, H.A. Bridgman, B.A. Bodhaine, S.J. Oltmans, and G.E. Shaw, Meteorology and haze structure during AGASP_II, part 1, Alaskan Arctic flights, 2-10 April 1986, *J. Atmos. Chem., 9,* 17-48, 1989.

Hobbs, P.V., A.L. Rangno, M. Shupe, and T. Uttal, Airborne studies of cloud structures over the Arctic Ocean and comparisons with retrievals from ship-based remote sensing measurements, *J. Geophys. Res.*, this issue.

Huebert, B.J., G. Lee, and W.L. Warren, Airborne aerosol inlet passing efficiency measurement, *J. Geophys. Res., 95,* 16,369-16,381, 1990.

Jayaweera, K.O.L.F. and T. Ohtake, Concentration of ice crystals in Arctic stratus clouds, *J. Res. Atmos., 7,* 199-207, 1973.

Kikuchi, K., M. Murakami, and Y. Sanuki, Preliminary measurements of the center nucleus of snow crystals using an energy dispersive X-ray microanalyzer, *Symp. Polar Meteorol. Glaciol., Tokyo, 4,* 157-174, 1982.

Kreidenweis, S.M., Y. Chen, D.C. Rogers, and P.J. DeMott, Isolating and identifying atmospheric ice-nucleating aerosols: A new technique, *Atmos. Res., 46,* 263-278, 1998.

Kumai, M., Identification of nuclei and concentrations of chemical species in snow crystals sampled at the South Pole, *J. Atmos. Sci., 33,* 833-841, 1976.

Langer, G., Evaluation of NCAR ice nucleus counter, part I, Basic operation, *J. Appl. Meteor., 12,* 1000-1011, 1973.

Markowitz, A., B. Raeymaekers, R. van Grieken, and F. Adams, Analytical electron microscopy of single particles, in *Physical and Chemical Characterization of Individual Airborne Particles*, edited by K.R. Spurny, John Wiley, New York, pp. 173-197, 1986.

Minnis, P., D.R. Doelling, V. Chakrapani, D.A. Spangenbert, L. Nguyen, R. Palikonda, T. Uttal, R. F. Arduini, and M. Shupe, Cloud coverage and height during FIRE ACE derived from AVHRR data, *J. Geophys. Res.*, this issue.

Murakami, M., K. Kikuchi, and C. Magono, Experiments on aerosol scavenging by natural snow crystals, part I, Collection efficiency of uncharged snow crystals for micron and sub-micron particles, *J. Meteor. Soc. Japan, 63,* 119-129, 1985.

Ohtake, T., K. Jayaweera and K.I. Sakurai, Observation of ice crystal formation in lower Arctic atmosphere, *J. Atmos. Sci., 39,* 2898-2904, 1982.

Okazaki, K. and K. Willeke, Transmission and deposition behavior of aerosols in sampling inlets, *Aerosol. Sci. Technol., 7,* 275-283, 1987.

Porter, J.N., A.D. Clarke, G. Ferry, and R.F. Pueschel, Aircraft studies of size-dependent aerosol sampling through inlets, *J. Geophys. Res., 97,* 3815-3824, 1992.

Radke, L.F., P.V. Hobbs, and J.E. Pinnons, Observations of cloud condensation nuclei, sodium-containing particles, ice nuclei and the light-scattering coefficient near Barrow, Alaska, *J. Appl. Meteorol., 15,* 982-995, 1976.

Radke, L.F., J.H. Lyons, D.A. Hegg, P.V. Hobbs, and I.H. Bailey, Airborne observations of Arctic aerosols, I, Characteristics of Arctic haze, *Geophys. Res. Lett., 11,* 393-396, 1984.

Rogers, D.C., Development of a continuous flow thermal gradient diffusion chamber for ice nucleation studies, *Atmos. Res., 22,* 149-181, 1988.

Rogers, D.C., Detecting ice nuclei with a continuous flow diffusion chamber — Some exploratory tests of instrument response, *J. Atmos. Oceanic Technol., 11,* 1042-1047, 1994.

Rogers, D.C., P.J. DeMott, S.M. Kreidenweis, and Y.Chen, Measurements of ice nucleating aerosols during SUCCESS, *Geophys. Res. Lett., 25,* 1383-1386, 1998.

Rogers, D.C., P.J. DeMott, S.M. Kreidenweis, and Y. Chen, A continuous-flow diffusion chamber for airborne measurements of ice nuclei, *J. Atmos. Oceanic Technol., 18,* 725-741, 2001.

Rosinski, J., P.L. Haagenson, C.T. Nagamoto, and F. Parungo, Ice-forming nuclei of maritime origin, *J. Aerosol Sci., 17,* 23-46, 1986.

Rosinski, J., P.L. Haagenson, C.T. Nagamoto, and F. Parungo, Nature of ice-forming nuclei in marine air masses, *J. Aerosol Sci., 18,* 291-309, 1987.

Schnell, R.C., Ice nuclei in seawater, fog water and marine air off the coast of Nova Scotia: Summer 1975, *J. Atmos. Sci., 34,* 1299-1305, 1977.

Schnell, R.C., Arctic haze and the Arctic Gas and Aerosol Sampling Program (AGASP), *Geophys. Res. Lett., 11,* 361-364, 1987.

Shaw, G.E., K. Stamnes, and Y.X. Hu, Arctic haze: Perturbation to the radiation field, *Meteorol. Atmos. Phys., 51,* 227-238, 1993.

Shupe, M.D., T. Uttal, S.Y. Matrosov, and A.S. Frisch, Cloud water contents and hydrometeor sizes during the FIRE Arctic Clouds Experiment, *J. Geophys. Res.*, this issue.

Szyrmer, W., and I. Zawadzki, Biogenic and anthropogenic sources of ice-forming nuclei: A review, *Bull. Am. Meteorol. Soc., 78,* 209-228, 1997.

Twomey, S., The influence of pollution on the shortwave albedo of clouds, *J. Atmos. Sci., 34,* 1149-1152, 1977.

Twomey, S., Aerosols, clouds and radiation, *Atmos. Env., 25A,* 2435-2442, 1991.

Wiedensohler, A., et al., Intercomparison study of the size-dependent counting efficiency of 26 condensation particle counters, *Aerosol Sci. Technol., 27,* 224-242, 1997.

Vali, G., Atmospheric ice nucleation — a review, *J. Rech. Atmos., 19,* 105-115, 1985.

P.J. DeMott and S.M. Kreidenweis, Department of Atmospheric Science, Colorado State University, Fort Collins, CO 80523. (pdemott@lamar.colostate.edu; soniak@aerosol.atmos.colostate.edu)

D.C. Rogers, NCAR/RAF, 10802 Airport Court, Broomfield, CO 80021. (dcrogers@ucar.edu)

(Received December 21, 1999; revised November 16, 2000; accepted November 29, 2000.)